Journal of Solid State Chemistry 213 (2014) 229–234

Contents lists available at ScienceDirect

Journal of Solid State Chemistry

journal homepage: www.elsevier.com/locate/jssc

Influence of the hydration by the environmental humidity on the metallic speciation and the photocatalytic activity of Cr/MCM-41

Verónica R. Elías [a], Ema V. Sabre [a], Elin L. Winkler [b], Leandro Andrini [c], Félix G. Requejo [c,d], Sandra G. Casuscelli [a], Griselda A. Eimer [a,*]

[a] Centro de Investigación y Tecnología Química (CITeQ) (UTN-CONICET), Maestro López esq. Cruz Roja Arg, Ciudad Universitaria, 5016 Córdoba, Argentina
[b] Centro Atómico Bariloche, CNEA-CONICET, Bustillo 9500, 8400 S. C. de Bariloche, Argentina
[c] Instituto de Fisicoquimica Teórica y Aplicada (INIFTA) (UNLP-CCT CONICET La Plata), 64 y Diag. 113, 1900 La Plata, Argentina
[d] Dto. de Física, Fac. de Ciencias Exactas, UNLP, La Plata, Argentina

ARTICLE INFO

Article history:
Received 12 December 2013
Received in revised form
12 February 2014
Accepted 1 March 2014
Available online 12 March 2014

Keywords:
Environmental humidity
Chromium species
TiO_2 cover
Photoactivity
MCM-41

ABSTRACT

The influence of the environmental humidity on the Cr species deposited on inorganic supports like MCM-41 silicates was analyzed by UV–vis Diffuse Reflectance (UV–vis RD), Electronic Spin Resonance (ESR) and X-ray near-edge (XANES) spectroscopy. Metal speciation could be inferred, finding that prolonged exposure periods under environmental humidity provoked the reduction of the active Cr^{6+} species and thus, the decrease of the Cr/MCM-41 photoactivity. After the Ti loading over the Cr modified samples, Cr species and the photoactivity were not notably influenced by the humidity exposure. Thus, it could be concluded that the presence of Ti is important because the TiO_2 cover protects the oxidized Cr species, stabilizing them.

1. Introduction

M41S family of mesoporous silicates and their transition metal derivatives, have been extensively studied in order to enhance their properties as environmental compatible catalysts [1–6]. In fact, the synthesis of mesoporous silicates with MCM-41 structure modified with transition metals has opened new possibilities in the catalysis area. In this sense, the molecular structure of metal oxides deposited on inorganic supports is of fundamental importance to understanding the behavior of these resulting composites as heterogeneous catalysts. Particularly, interesting results have been reached in photochemical processes, among which the photocatalytic degradation of organic compounds can be found [7–9]. Several metals were used in order to modify MCM-41 molecular sieves and give to them photocatalytic properties. In this regard, Cr showed a good performance in organic compounds degradation under visible radiation [9–12]. Nevertheless, Cr as a transitional metal of the 3d series presents a notable variability in their oxidation states, coordination number and molecular structure [13]. Thus, investigate the Cr species on inorganic oxide surfaces is of fundamental importance to understanding the behavior of Cr in Cr-based heterogeneous catalysts. The impregnation of a support with a Cr source (salt of Cr), followed by drying and calcination procedures, usually do not result in the thermodynamically more favored reaction that is the chromia (α-Cr_2O_3) formation [14]. This phenomenon is generally explained by the stabilization of Cr^{6+} species onto the support. However, the molecular structure of Cr species anchored on the surface, is strongly dependent on the environmental conditions. Thus, the presence of humidity in the environment where the catalyst is stored could have a notable influence on the Cr speciation and therefore, on the catalytic activity of the synthesized materials. In this sense, this work reports a study about the influence of the humidity on Cr speciation in MCM-41 materials and on their photoactivity in the azo-dyes degradation. This analysis has been performed by means of the combination of two spectroscopic techniques. Moreover, the effect of the loading of a second metal (Ti) on the stabilization of the active Cr species has been evaluated.

2. Experimental

2.1. Synthesis

The bare MCM-41 silicate was synthesized according to a previous report [15]. These silicates were modified with Cr by the wet impregnation method in order to reach metal loadings of

* Corresponding author. Tel./fax: +54 351 4690585.
E-mail address: geimer@scdt.frc.utn.edu.ar (G.A. Eimer).

http://dx.doi.org/10.1016/j.jssc.2014.03.002

3.5, 5.0 and 10.0 wt%, according to the previous report [10]. These solids were calcined at 500 °C for 9 h. The Cr modified MCM-41 were also modified with Ti using a solution of Ti *n*-butoxide in isopropanol and then calcined at 500 °C [10]. The nomenclature used was: TiO_2/Cr/MCM-41(x), where (x) is the theoretical Cr loading and TiO_2 indicates the Ti loading. These samples were referred as calcined samples. In order to investigate the effect of relative humidity (RH) on the photocatalytic activity of the solids, the calcined samples modified only with Cr and those modified with Cr and Ti, were then exposed for different periods to the atmospheric RH. According to the record of the meteorological station 873440 (SACO) from Argentina corresponding to the months from March to June of 2012, in which the experiments were made, the average values of RH were in the range between 69.5 and 52.2%. These samples were referred as hydrated samples. Then the samples were calcined again at 500 °C for 9 h, and referred as re-calcined samples.

2.2. Characterization

The Ti and Cr content in the final solids were determined by X-ray fluorescence (XRF) using an Innov-X System model ALPHA-4000. UV–vis RD spectra were measured in the wavelength range of 200–900 nm using a Jasco 650 spectrometer. The ESR spectra of the samples were recorder with a Bruker ESP 300 spectrometer operating at 9.5 GHz. The spectroscopic analyses were performed for the samples: calcined, hydrated (after the exposure to the environmental conditions) and re-calcined (after a new calcination of the hydrated samples at 500 °C for 9 h).

The Cr K XANES spectra were recorded at the XAFS2 beamline of the *Laboratorio Nacional de Luz Sincrotron* (LNLS, Campinas, Brazil) [16], running in storage ring mode at 1.37 GeV and with an average current of 250 mA. The synchrotron radiation beam was monochromatized by a double crystal Si(1 1 1) monochromator, with an energy resolution of 1.9 eV at the Cr K-edge. The photon flux was about 10^{10} photons/s for a beam size of about 450 × 250 μm^2.

The samples were prepared as a pellet and fixed between two self-adhesive Kapton tapes, after *ex situ* heating treatment in air at 500 °C in a tubular furnace for 9 h. The spectra were recorded in transmission mode with ionization chambers filled with N_2/Ar_2 mixture under appropriate pressure for optimal absorption. Between the second and the third ionization chamber was placed a Cr metallic foil for energy calibration purposes.

The data processing was performed by standard procedures using the Athena software [17].

2.3. Photocatalytic evaluation

The degradation experiments of the azo-dye Acid Orange 7 (AO7) in aqueous solution were performed using the photoreactor and the experimental conditions already described in our previous reports [10,11]. The AO7 concentration was monitored at 485 nm using a Jasco 7800 spectrometer. The degradation percentage was calculated as $X=(C_0-C)/C_0$, where C_0 is the concentration after to reach the adsorption/desorption equilibrium in the dark.

3. Results and discussion

The already reported XRD patterns of the calcined samples are typical of the MCM-41 structure with the presence of the hexagonal ordered unidirectional channels [11]. The XRD patterns of the hydrated and re-calcined solids are similar to the already reported. Table 1 shows the chemical composition and the structural properties of the synthesized catalysts as it was reported in [11].

Table 1
Chemical composition and structural properties of the synthesized catalysts.

Catalyst	Ti[a] (wt%)	Cr[a] (wt%)	Dp[b] (nm)	Vp[c] (cm^3/g)	Area[d] (m^2/g)
Cr/MCM-41(3.5)	–	2.05	2.52	1.353	1071
Cr/MCM-41(5)	–	2.90	2.63	1.451	1045
Cr/MCM-41(10)		6.51	2.54	1.624	1006
TiO_2/Cr/MCM-41(3.5)	22.17	1.34	2.33	1.868	741
TiO_2/Cr/MCM-41(5)	21.42	1.82	2.32	1.589	791
TiO_2/Cr/MCM-41(10)	25.52	3.455	2.46	1.637	706

[a] Measured by XRF.
[b] Pore diameter calculated by the BJH method.
[c] Pore volume.
[d] Surface area (BET).

A useful and very sensitive technique for the study of the different metallic species formed in the mesoporous structures is the ESR spectroscopy. Fig. 1 shows the spectra corresponding to the calcined, hydrated and re-calcined samples. Several signals with different characteristics can be identified in the spectra, as it was already reported in [18–21]. A narrow resonance, identified as γ, centered at a resonance field $H_r \sim 3410$ Oe and with peak to peak linewidth of $\Delta H \sim 20$ Oe, is observed in all the spectra corresponding to the calcined and re-calcined samples. This signal is assigned to isolated $Cr^{5+}(3d^1)$ ions dispersed in the matrix [22,23]. In addition, an inhomogeneously broadened signal, identified as β, with $\Delta H \sim 800$–1000 Oe and located at $H_r \sim 3400$ Oe is also observed. This absorption is assigned to dispersed Cr_2O_3 clusters. Finally, it is observed a narrower and an almost symmetric signal centered at $H_r \sim 3400$ Oe with $\Delta H \sim 300$ Oe, identified as κ by Puurunen et al. [24]. This signal is usually assigned to the presence of Cr^{3+} dispersed in the sieve or to amorphous Cr_2O_3 clusters. After the exposure of the calcined Cr/MCM-41(x) samples at environmental conditions notable changes in the spectra can be observed: the line assigned to Cr^{5+} (γ) diminishes in intensity, while the resonance of dispersed Cr^{3+} ions (κ) markedly increases. Then, after the re-calcination treatment the resonance of the oxidized Cr^{5+} species again increases and the signal corresponding to the dispersed Cr^{3+} ions diminishes. These results suggest that the exposure to the environmental humidity favors the reduction of the metallic species [25]. The changes are more noticeable when the Cr content of the samples increases; this behavior implies that the samples with high Cr content are more sensitive to the environmental humidity presence. Meanwhile, the solids modified with Ti show practically the same ESR spectra for the calcined, hydrated and re-calcined samples. This would be indicating that the TiO_2 is protecting the oxidized Cr species. Nonetheless, the behavior of the TiO_2/Cr/MCM-41(5) sample was slightly different. As it was already reported [18], this Cr content allows the appearance of a δ signal, assigned to the presence of surface isolated Cr^{3+} ions stabilized after Ti loading [24–26]. In this case, although these Cr species are protected by the titania cover, they are in the surface and, after applying the re-calcination process, can migrate and sinter, resulting in the appearance of the β signal corresponding to Cr_2O_3 clusters.

Then, UV–vis RD spectroscopy was employed in order to analyze the coordination environmental of the metallic species present in the MCM-41 structure (Fig. 2). It could be observed that the Cr/MCM-41(x) solids show absorption at 200–400 nm assigned to the charge transfer of O^{2-}–Cr^{6+} in monochromates $(CrO_4)^{2-}$. Then, the absorption in the 400–550 nm range corresponds to Cr^{6+} in di/polychromates, although an absorption at 450 nm could also be assigned to octahedral Cr^{3+} species present in small clusters [11,19,20]. Meanwhile, the absorption at wavelengths higher than 550 nm is assigned to Cr^{3+} in α-Cr_2O_3 nanoparticles [10,19,20,27–30]. For the TiO_2/Cr/MCM-41(x) samples, the

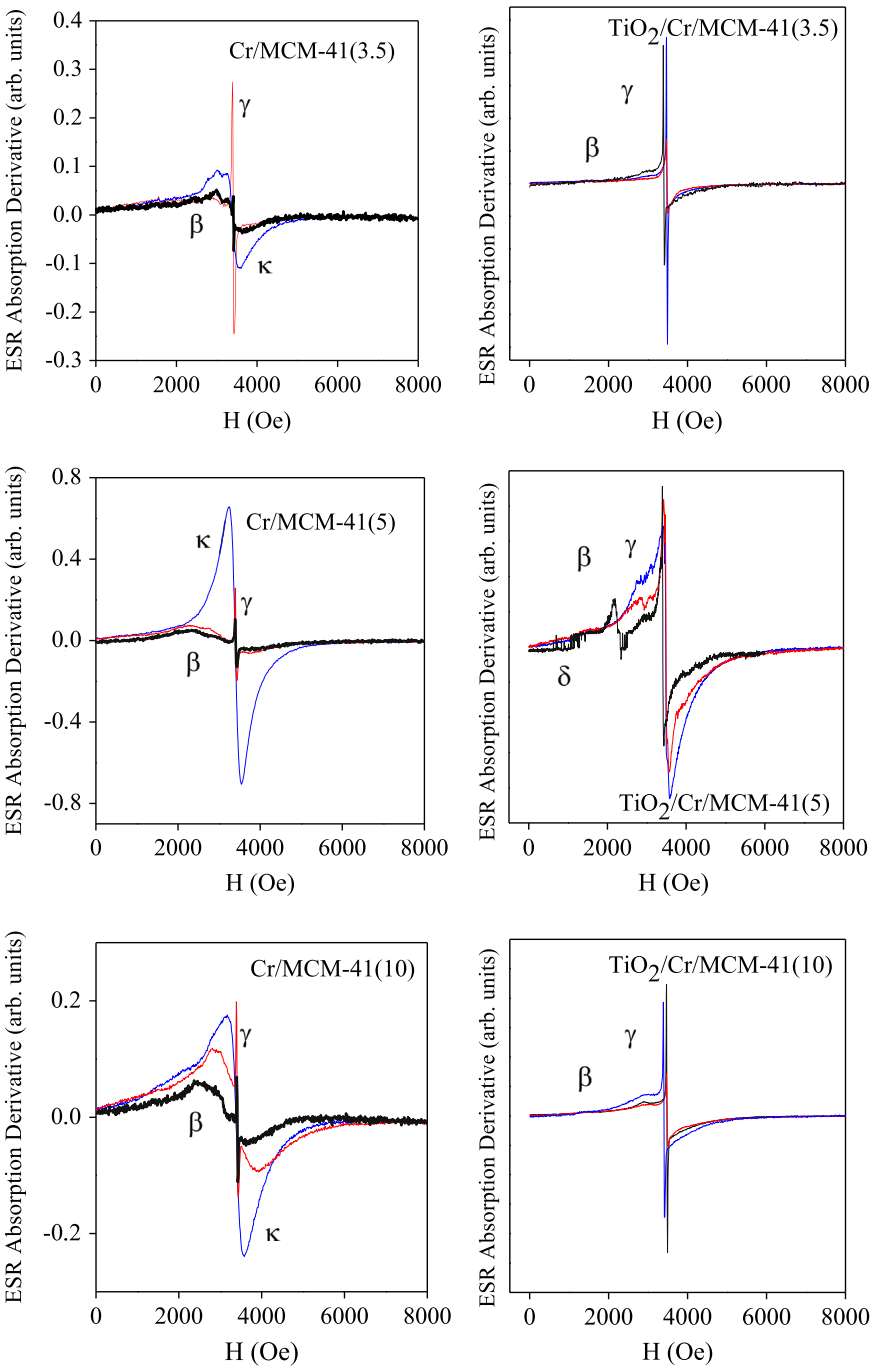

Fig. 1. ESR spectra of the calcined (black lines), hydrated (blue lines) and re-calcined (red lines) samples. (For interpretation of the references to color in this figure legend, the reader is referred to the web version of this article.)

absorption in the UV region can be awarded to the presence of titania (TiO_2), while the ability to absorb visible radiation is related to the Cr presence [9,12,31,32]. After the Ti loading, the samples with lower Cr content, show absorption in the 650–850 nm region which would be related to a synergistic effect between Cr and Ti. It has been already reported the importance of this heterojunction for the photocatalytic activity in these solids [9,11,32]. On the other hand, the differences in the ability for absorb radiation between the hydrated and re-calcined samples can also be observed in Fig. 2. From these spectra, it is possible to infer that the re-calcination of the hydrated samples leads to the restitution of the absorption around 350 nm (associated to oxidized Cr species (Cr^{6+}), observed for the calcined samples [11,19,20,33]. On the other hand, the increase in the absorption above 550 nm, very notable for the sample with the highest Cr loading (Cr/MCM-41(10)), could be associated to the higher amount of α-Cr_2O_3 nanoparticles, as consequence of a sintering effect by the re-calcination process. Meanwhile, Fig. 2B shows that the spectra of the samples modified with Ti are not affected by the environmental humidity exposure, being practically equivalent to those obtained after applying the re-calcination process.

XANES spectra are frequently used as a "fingerprinting" to recognize, for instance, in a straightforward way a tetrahedral coordination from an octahedral one [34] and changes in the average oxidation states [35,36]. An important XANES feature for all 3*d* transition elements is the pre-edge peaks structure [37].

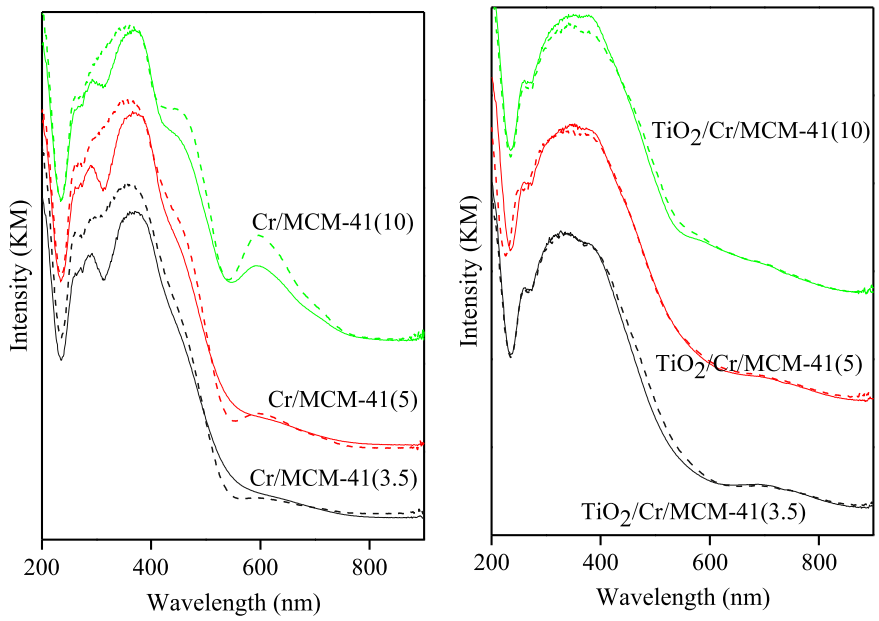

Fig. 2. UV–vis RD spectra of the hydrated (solid line) and the re-calcined (dash lines) samples.

The pre-edge peak intensity for absorbing atoms (probes) with T_d symmetry is larger than those for O_h symmetry [38], and the intense pre-edge peak for tetrahedral species of 3*d* transition metals is due to the *p* component at the final state of the transition with *d*–*p* hybridized orbital [38]. Additionally, for the Cr environment, is well known that tetrahedral coordination geometry only exists in Cr with the oxidation states 4+, 5+ and 6+, whereas under octahedral coordination only occurs with oxidation states 3+ and 4+ [39].

Cr K XANES spectra of reference compounds of metallic Cr, $K_2Cr_2O_7$ and Cr_2O_3 are reported in Fig. 3. In the corresponding *in-set*, the normalized the pre-edge peaks region for $K_2Cr_2O_7$ and for Cr_2O_3 are observed. As metallic compound, Cr has a numeral formal oxidation state "0", in cubic coordination geometry and Cr has tetrahedral coordination polyhedron in $K_2Cr_2O_7$ (Cr^{6+}) and octahedral coordination in Cr_2O_3 (Cr^{3+}). [40]. In the corresponding XANES spectra for these reference compounds, the differences in the intensity of the pre-edge peak is clearly observed. It is well known that the pre-edge peaks intensity decreases when increasing coordination numbers and the features of the pre-edge peak are strongly influenced by the symmetry of the coordination sphere [41].

Cr K XANES spectra of the synthetized Cr/MCM-41 samples are reported in Fig. 4. Considering the particular and clearly distinguishable features for Cr XANES spectra for Cr at 3+ or 6+, it is possible a rapid and qualitative evaluation of the Cr average oxidation state in each sample. Indeed, the characteristic feature of Cr^{6+} is a very high pre-peak intensity (at 5993 eV), being, in addition, clearly different at the white-line region (between 6000 and 6020 eV) from the corresponding spectrum for Cr^{3+} species, which not present pre-peak feature at all. The different content of Cr^{3+} and Cr^{6+} at the samples with different Cr concentration can be determined by the analysis of the weighted overlapping of the reference signals assigned to Cr in 3+ and 6+ pure oxidation states. Thus, the XANES signal corresponding to Cr^{6+} appears more intense for the sample with the lower Cr content, in which it is expected a higher amount of Cr ions in the higher oxidation state, according to the observed by UV–vis RD and ESR. Meanwhile, as the Cr loading is increased, the signal of Cr^{6+} decreases and that corresponding to Cr^{3+} increases becoming more defined their characteristics peaks. The enlarged presence of Cr^{3+} in the samples with higher Cr contents is consistent with the determination of the other techniques (UV–vis RD and ESR) which also showed the increment of Cr_2O_3. The corresponding linear fit of the XANES spectra by superimposition of reference spectra (Cr^{6+} and Cr^{3+}) is showed in Fig. 4 and the fitted values are reported in Table 2. Finally, by means of ESR, UV–vis RD and XANES the chemical state of Cr^{6+}, Cr^{5+} and Cr^{3+} ions present in the catalysts could be identify.

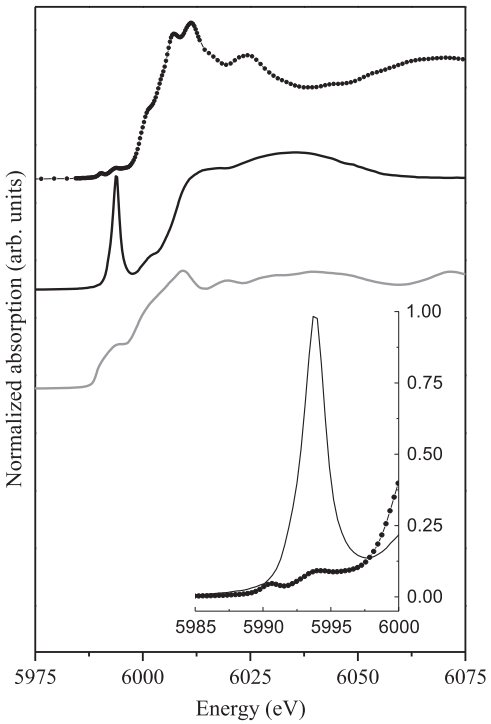

Fig. 3. The normalized Cr K XANES spectra for reference compounds: Cr metallic (gray solid line), $K_2Cr_2O_7$ (black solid line) and Cr_2O_3 (dash–dot). In the *in-set*: normalized pre-edge peaks for $K_2Cr_2O_7$ and for Cr_2O_3.

In our previous report it was corroborated that the oxidized Cr species are the photoactive ones for the azo-dye degradation [11]. Here, the effect of the hydration on the catalysts activity could be

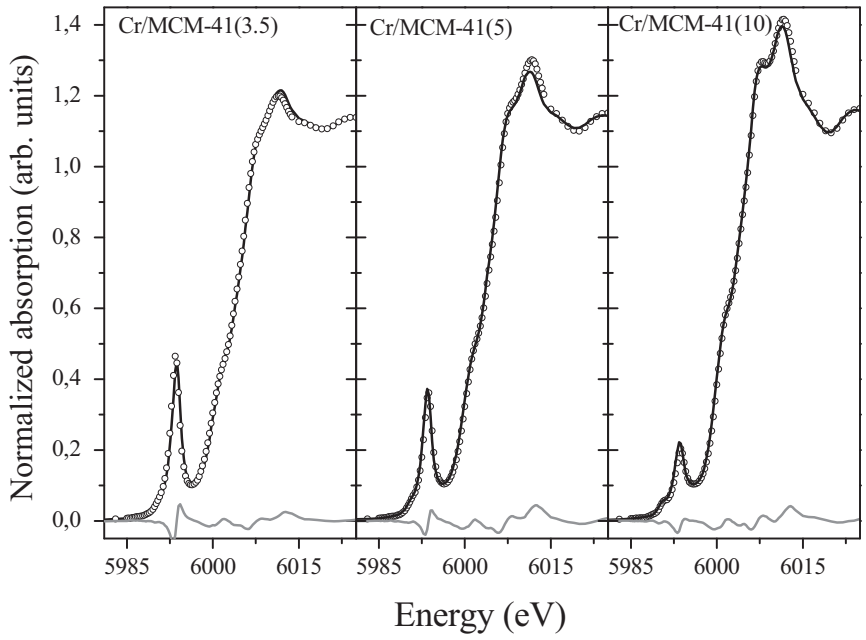

Fig. 4. The normalized Cr K XANES spectra for calcined Cr/MCM-41 samples. The dot is experimental spectra, the black solid line is the best linear combination fit using Cr K XANES of reference compounds (Cr^{3+} and Cr^{6+}) and the gray solid line is the difference between experimental and fitting spectra (error).

Table 2
Chromium Cr^{3+} content (%) present in each sample obtained by Cr K XANES linear combination fitting of reference compounds (Cr^{3+} and Cr^{6+}).

Catalyst	Cr^{3+} (%)[a]
Cr/MCM-41(3.5)	22.0 ± 0.6
Cr/MCM-41(5)	24.5 ± 0.1
Cr/MCM-41(10)	36.2 ± 0.7

[a] The Cr^{6+} is obtained as $100 - [Cr^{+3}]$.

Table 3
Catalytic activity of the solids exposed to the environmental humidity for different periods.

Catalyst	X (%)	Exposure period (days)
Cr/MCM-41(3.5)	67.36	0
Cr/MCM-41(3.5)	63.25	3
Cr/MCM-41(3.5)	56.56	8
Cr/MCM-41(5)	69.29	0
Cr/MCM-41(5)	58.50	3
Cr/MCM-41(5)	45.70	8
Cr/MCM-41(10)	80.95	0
Cr/MCM-41(10)	61.05	3
Cr/MCM-41(10)	43.00	8
Cr/MCM-41(10)	27.00	18
TiO_2/Cr/MCM-41(3.5)	78.76	0
TiO_2/Cr/MCM-41(3.5)	76.86	3
TiO_2/Cr/MCM-41(3.5)	79.50	8
TiO_2/Cr/MCM-41(5)	66.52	0
TiO_2/Cr/MCM-41(5)	63.89	3
TiO_2/Cr/MCM-41(5)	57.77	8
TiO_2/Cr/MCM-41(10)	79.37	0
TiO_2/Cr/MCM-41(10)	74.80	3
TiO_2/Cr/MCM-41(10)	68.00	8

explained from the spectroscopic analysis. In this sense, it can be observed in Table 3 that the activity of the Cr/MCM-41(10) sample is strongly dependent on the environmental humidity exposure. Thus, after calcination, this catalyst leads to 80% of AO7 degradation which is notably reduced to 27% after 18 days of humidity exposure. Then, this catalyst recovers its activity after the re-calcination process giving account for the recovering of the active oxidized Cr species. The effect of the hydration is notably minor for the catalysts with lower Cr content, probably because the oxidized Cr species, in lower amount, are more dispersed and less exposed. When the catalysts were also modified with Ti, the influence of the humidity on the solids activity was practically negligible. In this sense, after 3 days of exposure to environmental conditions, the catalyst without Ti loading (Cr/MCM-41(10)) shows an activity reduction of around 50%, while the activity of the Ti loaded catalyst (TiO_2/Cr/MCM-41(10)) remain practically unchanged.

The results of the spectroscopic characterization and the photocatalytic tests for our Cr modified MCM-41 catalysts could be explained taking account that after the impregnation of the molecular sieve with an aqueous solution of Cr, the Cr^{3+} ions are present as hexaaquo complexes. The location and nature of these complexes after impregnation is not known, but appreciable quantities of Cr may be inside the channels on the surface of the pore walls. Upon calcination, the water molecules are removed and Cr^{3+} ions are mainly oxidized. The formed dehydrated species can be anchored by an esterification reaction with the hydroxyl groups of the MCM-41 resulting in the formation of the surface Cr species such as chromate or di/polychromate (Cr^{6+}), chromyl cations (Cr^{5+}), and some Cr_2O_3 clusters (Cr^{3+}).

On the other hand, under hydration conditions [13,42], the surface of inorganic supports is covered by a thin water film and the hydroxyl population on this surface is subject to pH-dependent equilibria reactions, which are detailed below:

$$Si\text{–}OH_2^+ \leftarrow\rightarrow Si\text{—}OH + H_s^+$$

$$Si\text{–}OH \leftarrow\rightarrow Si\text{—}O^- + H_s^+$$

$$H_s^+ \leftarrow\rightarrow H^+$$

where H_s^+ and H^+ represent the surface and solution proton, respectively. It is important to note that the isoelectric point (IEP) (pH at which the surface of the support has a net zero charge) is dependent on the support type and that at lower IEP the

equilibrium of the reactions is driven to right. Therefore, MCM-41 silicates (which IEP reported in literature is between 3 and 4.6 [13,43]), present a higher H^+ concentration near the surface. Then, for samples modified with Cr by impregnation, the decrease in the surface pH by the hydration favors the polymerization of the oxidized Cr species. At the same time, under these acidic conditions, the highly polymerized Cr^{6+} species tend to be reduced and the following reaction is involved:

$$Cr_2O_7^{2-} + 14H^+ + 6e^- \leftarrow\rightarrow 2Cr^{3+} + 7H_2O \quad E_0 = 1.33 \text{ eV}$$

where Cr^{3+} ions would be present, mainly, as octahedral hexaaquo ions $Cr(H_2O)_6^{3+}$ highly dispersed in the sieve.

All the mentioned is in agreement with the observed by us through the spectroscopic analysis. From these observations it is possible to infer the cause of the low activity observed for the hydrated catalysts. Thus, the hydrated surface of the solids exposed to the environmental humidity leads to the presence of the κ signal in the ESR spectra, typical of hydrated Cr^{3+} complexes. After the re-calcination process, this signal disappears and a signal corresponding to oxidized Cr species emerges (γ). At the same time, an increase in the absorption corresponding to the monochromates (Cr^{6+}) is observed in the UV–vis RD spectra, after re-calcination of the hydrated samples. Thus, the environmental humidity would provoke the reduction of the oxidized Cr species (present after the impregnation and calcination process) to Cr^{3+} species inactive for the photocatalytic degradation of organic compounds [11]. Therefore, it could be corroborated that the notably major activity observed in the catalysts after the first calcination and re-calcination processes is attributed to the incremented presence of active oxidized Cr species. On the other hand, the photoactivity corresponding to the catalysts also modified with Ti was not affected by the environmental humidity. These results are in agreement with the spectroscopic analysis that showed that the metallic speciation was not changed by exposure to the environmental conditions when Ti is present in the catalysts. These observations evidence the shielding effect of the TiO_2 cover on the oxidized Cr species, protecting them from the water presence. Finally, it could be concluded that the Ti is important to increase the photoactivity through a synergistic effect (mainly for samples with lower Cr loadings [11]) and to stabilize the oxidized active Cr species (mainly for samples with higher Cr loadings).

4. Conclusions

By a combined spectroscopic analysis, it could be evidenced the presence of oxidized Cr species (Cr^{6+} and Cr^{5+}) in the calcined and re-calcined samples and of reduced Cr species in the hydrated samples. On the other hand, a longer exposure to the environmental humidity led to a major decrease in the activity, mainly for the higher Cr loaded samples. These results would be associated to the reduction of the active Cr species under hydration. Thus, the hydroxyl groups in the support surface are subject to several reactions that tend to the formation of hydrated Cr^{3+} complexes, from the chromates present in the surface. Moreover, under hydration conditions, the Ti loading avoids the decrease in activity of the catalysts modified with Cr. This evidences the importance of this second metal to protect the photoactive Cr species from the water presence and their consequent reduction.

Acknowledgments

The authors are grateful to UTN-FRC and CONICET for the financial support.

References

[1] M. El-Naggar, R. Aglan, M. Sayed, J. Environ. Chem. Eng. 1 (3) (2013) 516–525.
[2] J. Jeon, H. Kim, S. Woo, Appl. Catal., B 44 (2003) 311–323.
[3] J. Bing, L. Li, B. Lan, G. Liao, J. Zeng, Q. Zhang, X. Li, Appl. Catal., B 115–116 (2012) 16–24.
[4] S. Idris, C. Davidson, C. McManamon, M. Morris, P. Anderson, L. Gibson, J. Hazard. Mater. 185 (2011) 898–904.
[5] F. Subhan, B. Liu, Y. Zhang, X. Li, Fuel Process. Technol. 97 (2012) 71–78.
[6] A. Di Paola, E. García-López, G. Marcì, L. Palmisano, J. Hazard. Mater. 211–212 (2012) 3–29.
[7] S. Rodrigues, K. Ranjit, S. Uma, I. Martyanov, K. Klabunde, J. Catal. 230 (2005) 158–165.
[8] M. Satuf, R. Brandi, A. Cassano, O. Alfano, Appl. Catal., B 82 (2008) 37–49.
[9] L. Davydov, E. Reddy, P. France, P. Smirniotis, J. Catal. 203 (2001) 157–167.
[10] V. Elías, E. Vaschetto, K. Sapag, M. Oliva, S. Casuscelli, G. Eimer, Catal. Today 172 (2011) 58–65.
[11] V. Elías, E. Sabre, K. Sapag, S. Casuscelli, G. Eimer, Appl. Catal., A 413–414 (2012) 280–291.
[12] B. Sun, E. Reddy, P. Smirniotis, Appl. Catal., B 57 (2005) 139–149.
[13] B. Weckhuysen, I. Wachs, R. Schoonheydt, Chem. Rev. 96 (1996) 3327–3349.
[14] B. Weckhuysen, A. Verberckmoes, A. Buttiens, R. Schoonheydt, J. Phys. Chem. 98 (1994) 579–584.
[15] V. Elías, M. Crivello, E. Herrero, S. Csasuscelli, G. Eimer, J. Non-Cryst. Solids 355 (2009) 1269–1273.
[16] ⟨http://lnls.cnpem.br/xafs/beamlines/xafs2/⟩.
[17] B. Ravel, M. Newville, J. Synchrotron Radiat. 12 (2005) 537–541.
[18] V. Elías, E. Sabre, Elin Winkler, M. Satuf, E. Rodríguez-Castellón, S. Casuscelli, G. Eimer, Microporous Mesoporous Mater. 163 (2012) 85–95.
[19] Z. Zhu, M. Hartmann, E. Maes, R. Czernuszewicz, L. Kevan, J. Phys. Chem. B 104 (2000) 4690–4698.
[20] Z. Zhu, Z. Chang, L. Kevan, J. Phys. Chem. B 103 (1999) 2680–2688.
[21] S. Rodrigues, K. Ranjit, S. Uma, I. Martyanov, K. Klabunde, J. Catal. 230 (2005) 158–165.
[22] B. Weckhuysen, L. De Ridder, R. Grobet, R. Schoonheydt, J. Phys. Chem. 99 (1995) 320–326.
[23] M. Lezanska, G. Szymanski, P. Pietrzyk, Z. Sojka, J. Lercher, J. Phys. Chem. C 111 (4) (2007) 1830–1839.
[24] R. Puurunen, B. Weckhuysen, J. Catal. 210 (2002) 418–430.
[25] D. Cordischi, V. Indovina, M. Occhiuzzi, Appl. Surf. Sci. 4 (55) (1992) 233–237.
[26] S. Khaddar-Zine, A. Ghorbel, C. Naccache, J. Mol. Catal. A: Chem. 1–2 (150) (1999) 223–231.
[27] L. Zhang, Y. Zhao, H. Dai, H. He, C. Au, Catal. Today 131 (2008) 42–54.
[28] S. Shylesh, C. Srilakshimi, A. Singh, B. Anderson, Microporous Mesoporous Mater. 99 (2007) 334–344.
[29] Y. Ohishi., T. Kawabata, T. Shishido, K. Takaki, Q. Zhang, Y. Wang, K. Takehira, J. Mol. Catal. A: Chem. 230 (2005) 49–58.
[30] L. Liu, H. Li, Y. Zhang, Catal. Commun. 8 (2007) 565–570.
[31] J. Pedraza-Avella, R. López, F. Martínez-Ortega, E. Páez-Mozo, R. Gómez, J. Nanopart. Res. 5 (2009) 95–104.
[32] S. Reddy Inturi, T. Boningari, M. Suidan, P. Smirniotis, J. Phys. Chem. C 118 (2014) 231–242.
[33] V. Elías, E. Vaschetto, K. Sapag, M. Crivello, S. Casuscelli, G. Eimer, Top. Catal 54 (2011) 277–286.
[34] A. Mottana, J. Robert, A. Marcelli, G. Giuli, A. Della Ventura, E. Paris, Z. Wu, Am. Mineral. 82 (1997) 497–502.
[35] T. Capehart, J. Herbst, R. Mishra, F. Pinkerton, Phys. Rev. B: Condens. Matter 52 (1995) 7907–7914.
[36] C. Engemann, J. Hormes, A. Longen, K. Dötz, Chem. Phys. 237 (1998) 471–481.
[37] L. Grunes, Phys. Rev. B: Condens. Matter 27 (1983) 2111–2131.
[38] T. Yamamoto, X-Ray Spectrom 37 (2008) 572–584.
[39] A. Pantelouris, H. Modrow, M. Pantelouris, J. Hormes, D. Reinen, Chem. Phys. 300 (2004) 13–22.
[40] F. Requejo, J. Ramallo-López, R. Rosa-Salas, J. Domínguez, J. Rodríguez, J. Kim, R. Quijada, Catal. Today 10–108 (2005) 750–758.
[41] F. Farges, G.E. Brown Jr, J.J. Rehr, Phys. Rev. B: Condens. Matter 56 (1997) 1809–1819.
[42] G. Parks, Chem. Rev. 65 (1965) 177–198.
[43] D. Sanchez-Alvarado, R. Silva-Rodrigo, A. Guevara-Lara, A. Castillo-Mares, A. Reyes-de la Torre; Influencia del pH en la preparación de catalizadores NiMo/MCM-41/Al_2O_3 en la Hidrodesulfuración de Dibenzotiofeno; 2011. XII Congreso Mexicano de Catálisis, Guanajuato, Gto.